Level density parameter study using a microscopic model

A. N. Behkami*
Radiation Center, Oregon State University, Corvallis, Oregon 97331

Z. Kargar and N. Nasrabadi
Physics Department, Shiraz University, Shiraz 71454, Iran
(Received 2 January 2002; published 5 December 2002)

Nuclear level density parameter a has been calculated over a large range of nuclear mass and energy, using the microscopic model with the inclusion of nuclear pairing interaction. The values of a and the energy shift parameter δ, appearing in the Bethe formula, are obtained by fitting the entropy as a function of excitation energy. Although the general behavior of a, obtained with nuclear entropy is very similar to that of the conventional Fermi gas model, it shows deviations in the vicinity of major nuclear shells. The dependence of the level density parameter on energy has also been investigated and it is shown that the variation of a at lower energy is significant and has an asymptotic approach to a constant a at higher energies. The dependence of a on pairing force and deformation is illustrated.

DOI: 10.1103/PhysRevC.66.064307 PACS number(s): 21.10.Ma

I. INTRODUCTION

Nuclear level density is an important quantity in the nuclear reaction theory. For years the Fermi gas model has been used to interpret experimental observations of level densities. To explain some of the gross deviations from the simple model, modifications have been introduced into the theory to include pairing and shell effects. In order to obtain agreement between theory and experiment, some of the level density data need an arbitrary adjustment of energy independent parameters in the theory. In particular, the back-shifted Fermi gas model has been introduced to obtain a simultaneous fit of observed level densities at low, medium and higher energies [1–4]. In this model, the quantity δ is an adjustable parameter used to account for pairing and shell corrections. It also defines the energy of a fictitious ground state with respect to the actual ground state. This model is reasonably successful in reproducing level densities of nuclei away from major shells. It has been known for some time that the experimental level density parameter a deviates considerably from the magnitude and constancy predicted by the Fermi gas model in the vicinity of major shells. Thus, the theory with energy independent parameters is not valid in all mass regions, and the theoretical parameters cannot be calculated directly.

In our previous publications [5,6] we have studied 75 nuclei, between ^{20}F and ^{250}Cf, and determined the parameters appearing in the Bethe level density formula. We have shown that a does not have a smooth mass dependence; it rather varies with the mass number, especially for nuclei near major nuclear shells.

A systematic study of the behavior of the nuclear level density parameter across a large mass region and energy has been a topic of interest from both theoretical and experimental viewpoints. Recently, there have been several attempts to obtain the temperature dependence of a in various approximations [7–12]. At sufficiently high excitation energies where the shell effects disappear, a simple linear mass dependence of a has been reported [13]. Most recently, a functional form of a as a function of energy and mass number has also been suggested [14].

In this study, we have used a microscopic model to deduce the level density parameter and examine its dependence on energy and mass number in more detail. The primary goal is to find more realistic values for the level density parameter, which is often employed in equilibrium decay calculations. In addition, we have studied the general behavior of a for a wide range of mass and temperature using the model calculations. The methods of calculations are illustrated in Sec. II and results of the calculations are discussed and outlined in Sec. III.

II. STATISTICAL CALCULATIONS OF LEVEL DENSITY PARAMETER

This section is a brief review of the microscopic model used to calculate the state density and level density parameters. The calculation procedure for the state density is outlined in our previous papers (Refs. [15,16]).

In the framework of statistical mechanics, the state density is defined as

$$\omega(N,E)=\frac{\exp(S)}{2\pi|D|^{1/2}}. \tag{1}$$

D is the determinant of the second derivatives of the grand partition function taken at the saddle point. At this stationary point the entropy S is given by

$$S=2\sum_k \ln[1+\exp(-\beta E_k)]+2\beta\sum_k \frac{E_k}{1+\exp(-\beta E_k)}, \tag{2}$$

where β is the inverse nuclear temperature and λ is related to chemical potential. $E_k=[(\epsilon_k-\lambda)^2+\Delta^2]^{1/2}$ is the quasi-

*On leave from Shiraz University, Shiraz, Iran.

particle energy, where ϵ_k is the energy of a single particle k, and Δ is the gap parameter that is a measure of nuclear pairing.

The saddle point conditions that must be satisfied are

$$\sum_k n_k = N, \tag{3}$$

$$\sum_k n_k \epsilon_k = E. \tag{4}$$

The occupational probability of level k is

$$n_k = 1 - \frac{\epsilon_k - \lambda}{E_k} \tanh \frac{\beta E_k}{2}. \tag{5}$$

For a system of N neutrons and Z protons, the total energy is given by

$$E = E_p + E_n \tag{6}$$

and the total entropy is given by

$$S = S_p + S_n. \tag{7}$$

The total level density for a system of N neutrons and Z protons at an excitation energy of $U = U_p + U_n$ is

$$\rho(N,Z,U) = \frac{\omega(N,Z,U)}{(2\pi\sigma^2)^{1/2}} \tag{8}$$

where σ^2 is the spin cutoff factor defined as

$$\sigma^2 = \sigma_p^2 + \sigma_n^2 \tag{9}$$

with

$$\sigma_n^2 = \frac{1}{2} \sum_k m_k^2 \sinh^2(1/2\beta E_k), \tag{10}$$

and a similar relation for σ_p^2.

The measure of exponential growth of the level density due to the shifted Bethe formula [17] is

$$\rho(E) = \frac{e^{2\sqrt{a(U-S)}}}{\sqrt{48}a^{1/4}(U-\delta)} \propto \frac{e^S}{\sqrt{D}}, \tag{11}$$

where a is approximately defined by

$$a = \frac{S^2}{4(U-\delta)}, \tag{12}$$

U designates the excitation energy, and δ is an energy shift parameter.

The steps necessary to calculate S_n are as follows: For a set of single particle levels and a particular choice of temperature T, the parameters λ and Δ are estimated and a set of occupational probabilities is calculated using Eq. (5). Next, the saddle point conditions are checked for a given nucleon number using Eq. (3). If the conditions are not met, the values of λ and Δ are adjusted and the procedure is repeated until the saddle point conditions are satisfied. Once the proper sets of n_k values are computed, the entropy S_n is calculated using Eq. (2). The energy E_n is calculated by applying Eq. (4) at a particular temperature T. The excitation energy U_n is then determined by subtracting the energy at $T=0$. The quantities σ_n^2, $\omega(N,E)$ are calculated using Eqs. (1) and (10). A similar set of calculations is used to calculate U_p and S_p for proton elements. Total entropy S, at excitation energy $U = U_n + U_p$, is then determined from Eq. (7) and the total level density is calculated using Eq. (8).

The square of the entropy is then plotted as a function of excitation energy. Straight line fit to the quantity S^2 as a function of U is performed at high energy regions, where the shell correction is rather constant. The value of the level density parameter a is determined from the slope using Eq. (12). The extrapolation of this straight line fit results in an intercept value of the energy shift parameter, δ.

III. SUMMARY AND RESULTS

Systematic studies of the behavior of the nuclear level density parameter in nuclei from ^{20}F to ^{250}Cf were performed. The investigation included a balanced number of *e-e*, *o*, *o-e*, light, medium, heavy, spherical, and deformed nuclei.

We have computed the state density and entropy for all nuclei listed in Table I as outlined in Sec. II. The single particle levels of Nilsson *et al.* [18] for deformed nuclei, and Seeger and Howard [19] in the case of spherical nuclei were used in the calculations. The initial values of the ground state gap parameters Δ_n and Δ_p used to fix the pairing strength were taken from Nix *et al.* [20,21].

For the odd particle system, relevant statistical functions were calculated for the adjacent doubly even nucleus and then the energy scale was shifted by an energy equivalent to that required to produce one quasiparticle.

In performing calculations of the level density for lanthanide and actinide nuclei, however, single particle energies and spins were first calculated for a specified deformation using the Nilsson potential, and then the state density and entropy as a function of excitation energy were evaluated.

The total entropy for each nuclear system was calculated as outlined in Sec. II. The square of entropy as a function of excitation energy for the ^{207}Pb nucleus is shown in Fig. 1. Similar curves plotted for the ^{210}Bi and ^{236}U nuclei are shown in Fig. 2. At higher energies, the vanishing of the shell effect is apparent, as the slope remains almost constant. It should be emphasized that whenever statistical properties of nuclei play a decisive role in nuclear reactions, the mentioned phenomena has an important consequence.

Figure 3 shows entropy curves for the ^{236}U nucleus at four different deformations. These curves have nearly the same slope in the (40–80)-MeV energy range. However, they show structures at lower excitation energies due to pairing interaction. The effect of pairing force decreases with increasing deformation and it becomes much smaller at larger deformations. The dependence of calculations on de-

TABLE I. Level density parameters of the Bethe and BCS model with their energy-shift values.

Nuclei	a (MeV)$^{-1}$ [a]	E_1 (MeV)	a (MeV)$^{-1}$ [b]	δ (MeV)
^{20}F	2.46	1.6(11)	4.00	3.01
^{22}Na	1.80	−5.3(77)	2.90	2.04
^{24}Na	2.60	−3.0(16)	3.05	3.18
^{24}Mg	4.20	5.5(19)	3.12	2.70
^{25}Mg	2.30	−1.8(19)	3.12	2.76
^{26}Mg	3.00	1.3(11)	3.09	3.44
^{28}Al	3.00	−1.9(13)	3.44	3.96
^{28}Si	2.60	2.9(5)	3.45	4.90
^{29}Si	4.80	3.5(7)	3.61	3.25
^{30}Si	2.50	0.3(25)	3.80	3.47
^{33}S	3.40	−0.3(9)	4.23	3.51
^{34}S	3.50	1.3(8)	4.43	1.83
^{36}Cl	3.70	−1.0(9)	4.68	1.03
^{40}K	4.60	−1.2(6)	5.29	2.70
^{41}K	5.39	−0.4(3)	5.32	1.73
^{40}Ca	3.60	2.2(27)	5.24	1.93
^{41}Ca	4.85	0.2(5)	5.43	2.38
^{46}Sc	5.64	−2.1(4)	5.59	1.59
^{55}Fe	5.30	−0.05(59)	6.89	2.87
^{60}Co	6.77	−1.24(25)	7.56	2.12
^{61}Ni	6.10	−0.7(4)	7.70	4.60
^{67}Zn	7.85	−0.62(31)	6.65	2.30
^{75}Se	9.75	−1.09(24)	9.74	0.98
^{77}Se	9.52	−1.05(31)	10.07	2.31
^{87}Sr	9.92	0.90(27)	10.17	1.79
^{95}Mo	9.82	−0.29(29)	12.23	2.04
^{96}Mo	10.19	0.71(27)	12.02	2.04
^{102}Ru	12.77	0.81(23)	13.04	1.39
^{106}Pd	13.09	0.84(15)	13.53	1.06
^{109}Pd	13.60	−1.01(20)	13.99	1.97
^{112}Cd	13.45	0.85(20)	14.22	1.90
^{114}Cd	14.48	1.21(12)	14.41	2.26
^{116}In	15.07	−0.68(15)	14.65	2.73
^{122}Sb	14.51	−0.95(15)	15.30	3.49
^{124}Sb	13.64	−1.09(16)	15.45	4.55
^{128}I	13.63	−1.43(15)	15.84	2.01
^{134}Cs	12.75	−1.40(13)	16.50	3.96
^{151}Sm	18.93	−0.66(15)	18.89	0.60
^{152}Sm	18.57	0.37(12)	18.61	2.09
^{153}Sm	17.11	−0.89(12)	18.64	−2.71
^{155}Sm	16.29	−0.59(15)	18.77	1.99
^{152}Eu	19.25	−1.48(9)	15.45	4.55
^{153}Eu	18.15	−0.54(14)	15.45	4.55
^{154}Eu	18.63	−1.31(7)	19.20	−1.01
^{153}Gd	18.84	−0.85(11)	18.86	3.20
^{155}Gd	19.34	−0.46(13)	19.36	1.41
^{156}Gd	18.00	0.52(11)	18.74	−0.69
^{158}Gd	17.41	0.48(8)	19.33	5.86
^{161}Dy	17.47	−0.66(13)	19.91	−6.51
^{168}Er	16.93	0.40(7)	20.48	−9.89
^{169}Er	16.66	−0.52(11)	20.40	−10.09
^{169}Yb	15.90	−0.67(12)	21.07	−4.05
^{172}Yb	17.68	0.41(8)	21.71	−9.91
^{174}Yb	17.44	0.63(16)	20.84	−10.83
^{178}Hf	18.26	0.36(9)	20.50	−3.24
^{179}Hf	18.26	−0.25(9)	21.92	−3.80
^{190}Os	18.72	0.48(12)	22.29	2.13
^{196}Pt	17.67	0.65(14)	22.31	3.16
^{198}Au	15.24	−1.27(14)	22.27	2.46
^{200}Hg	13.28	0.02(17)	22.37	2.18
^{207}Pb	9.6	1.23(44)	20.18	2.95
^{210}Bi	9.8	−0.76(34)	22.26	3.15
^{230}Th	23.40	0.13(10)	23.78	−4.39
^{231}Th	26.10	−0.24(8)	21.05	−10.65
^{234}U	24.02	0.40(6)	22.34	−6.78
^{235}U	24.10	−0.32(10)	23.18	−7.98
^{236}U	25.20	0.22(7)	21.58	−8.90
^{237}U	25.80	−0.20(13)	19.88	−13.92
^{239}U	24.02	−0.14(8)	22.34	−6.78
^{240}Pu	23.10	0.26(8)	22.34	−6.78
^{244}Am	26.60	−0.65(6)	29.81	−11.91
^{250}Cf	22.90	0.33(9)	19.69	−11.97

[a]Values deduced from the Bethe formula.
[b]Values obtained from the BCS model.

formation is shown in Fig. 4, where the logarithm of the state density is plotted as a function of energy for the ^{244}Am nucleus at various deformations. Figure 5 shows the dependence of nuclear temperature on energy at these deformations for the ^{244}Am nucleus. The effect of pairing interaction and phase transition is also apparent at lower excitation energies. The points for zero deformation $\epsilon=0$ lie above the points with nonzero deformations. This is expected within the Nilsson model as a result of the decreased single particle level density with increasing deformation.

The values extracted from the slope a and the intercept δ for all nuclei under investigation are listed in Table I. The

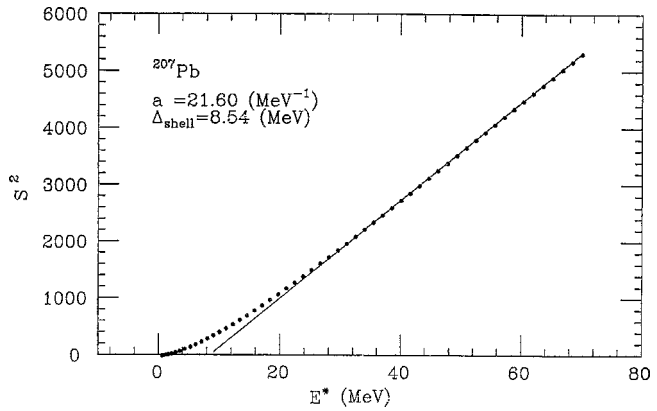

FIG. 1. Plot of the entropy squared versus excitation energy for ^{207}Pb with zero deformation. Note the straight line fit at higher energies.

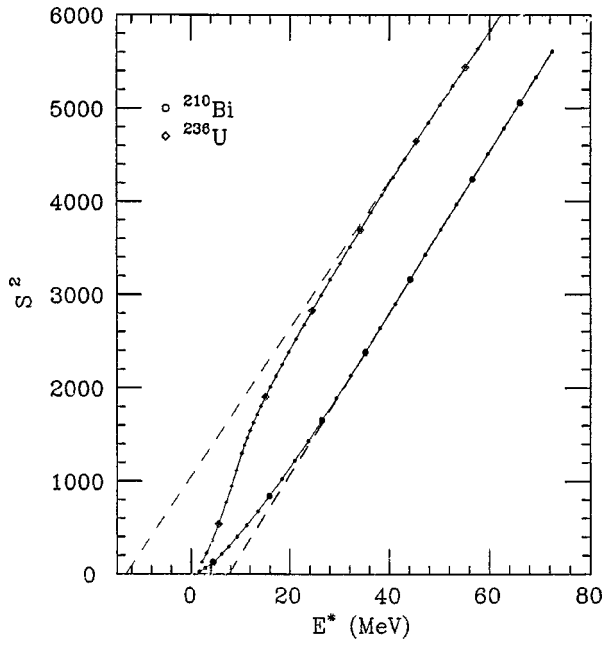

FIG. 2. Plot of the entropy squared versus excitation energy for ^{210}Bi and ^{236}U together with straight line fits at high energies.

level density parameter and energy shift δ deduced from the Fermi gas formula (see our previous publication, Ref. [6]) are also listed in Table I. The values of a in MeV^{-1} from two different calculations are plotted in Fig. 6 as a function of mass number for comparison. Examination of Fig. 6 reveals that the level density parameter obtained from the microscopic theory increases smoothly with mass number A. However, the corresponding values of a from the Fermi gas model show variations from the smooth A dependence. For the nuclei in the vicinity of major nuclear shells this deviation is substantial.

The dashed line in Fig. 6 represents a values given by $A/8$ MeV^{-1}, which is frequently employed in equilibrium decay calculations. One observes that a increases with A as expected theoretically. However, there are marked deviations from this smooth trend, especially for a values near closed shells. For example, in the vicinity of the $Z=82$, $N=126$

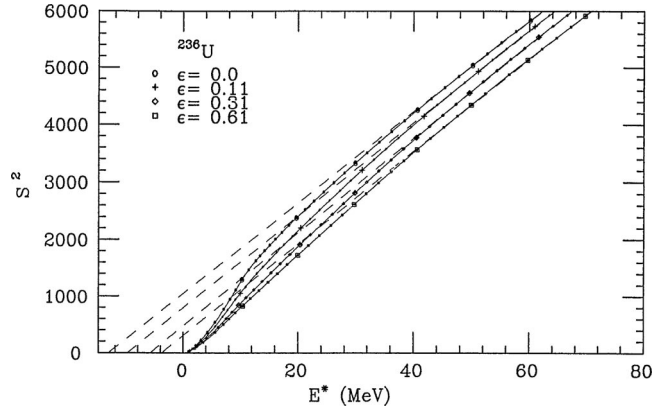

FIG. 3. Plot of the entropy squared for ^{236}U at four deformations with a straight line fit at each deformation.

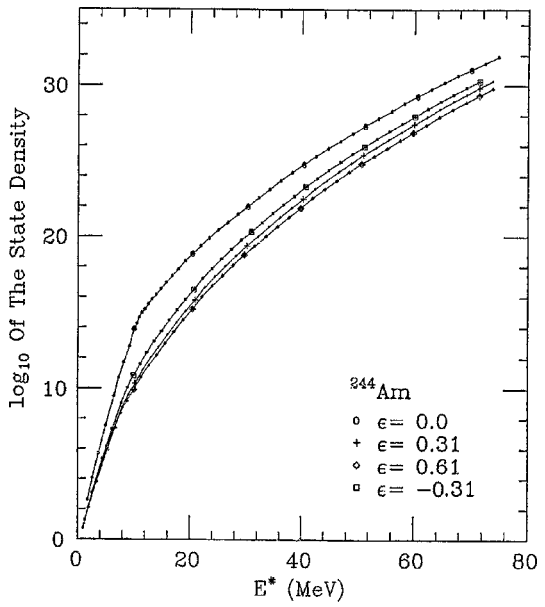

FIG. 4. Plot of the logarithm of the state density as a function of excitation energy for ^{244}Am at four deformations.

shells, a values are more than a factor of 2 smaller than those of nearby nuclei. Such irregularities are associated with the low single particle level densities near the Fermi energy for nuclei near closed shells. The thick line represents the general trend of the level density parameter obtained from the microscopic model to be compared with the dashed line. An interesting regularity emerges from the data listed in Table I and plotted in Fig. 6; the values of a from the statistical entropy calculations increase smoothly in all mass regions, and are significantly higher than their corresponding values from the Fermi gas model for nuclei near major shells.

The values from the present compilations were compared with those made by Ignatyuk *et al.* [22] and that of Huang

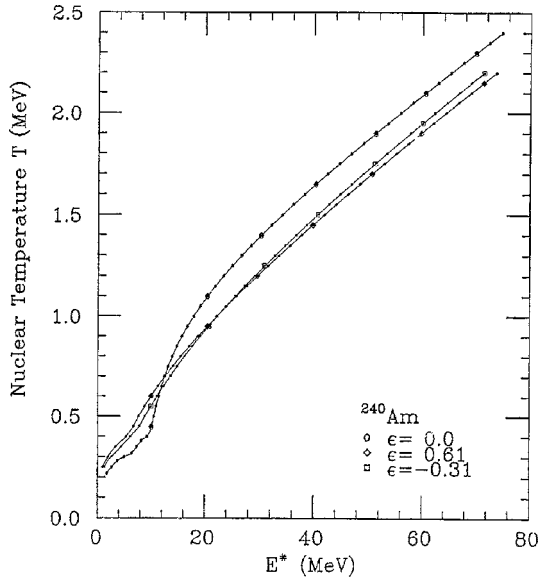

FIG. 5. The variation of nuclear temperature in MeV as a function of excitation energy for ^{244}Am at various deformations.

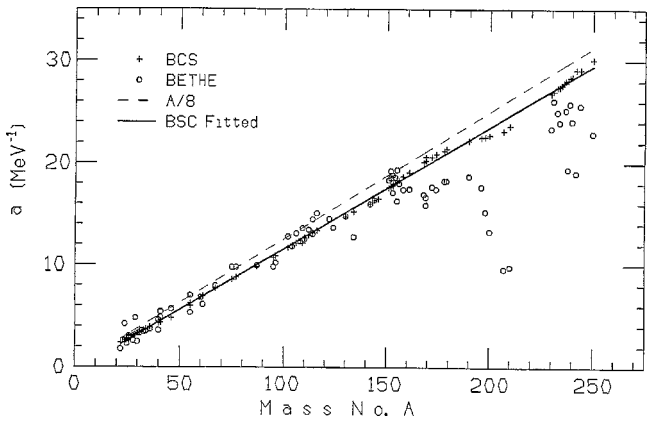

FIG. 6. Values of the level density parameter in MeV^{-1} as a function of mass number A from two different calculations. The parametrization $A/8$ MeV^{-1} is also plotted for comparison.

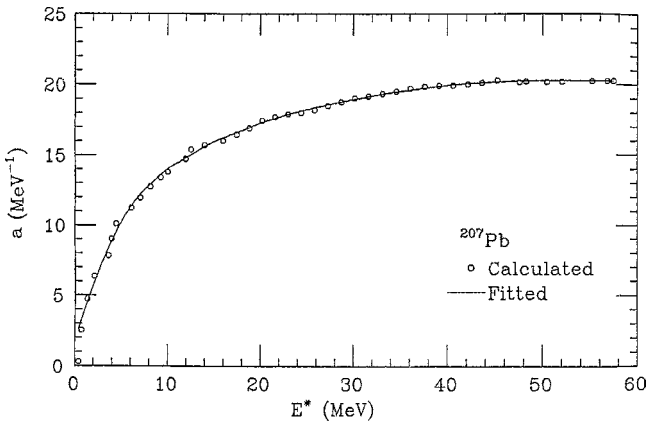

FIG. 7. Values of the level density parameter as a function of energy for ^{207}Pb extracted from Fig. 1. The curve through the calculated points is drawn to guide the eye.

et al. [23]. Although, the general trends are in qualitative agreement with those reported by these authors, they differ by about 15% for nuclei between the closed shells. This is perhaps not surprising because the level density increases with energy at a slower rate for closed shell nuclei.

To obtain an approximate energy dependent for a, we focus on the low energy portion of the entropy square curves for which the S^2 dependence on energy is not linear. The fit in this region is made by partitioning the energy range and by using the linear behavior of the square of the entropy with energy for each energy partition between subenergies. The slope a (U), deduced from the relation $S^2=4a(U)[U-\delta(U)]$, is plotted in Fig. 7 for the ^{207}Pb nucleus. We note a sharp increase in a with energy at lower excitation energies, but it changes slowly with energy and becomes almost constant at higher excitation energies. Similar behavior has also been observed for other nuclei studied. Although no theoretical predictions are available to give us the form, such energy dependence has been reported in dealing with shell effects [24–26].

In summary, in this paper we have presented more realistic calculations of the level density parameter for a wide range of mass region; and show that the parametrization $a=A/8$ MeV^{-1} is an approximation. It is completely inadequate near magic nuclei; instead, significant shell and pairing effects appear for these nuclei, and these effects manifest themselves by an associated decrease in the level density parameter with increasing mass number.

ACKNOWLEDGMENTS

We are indebted to the Radiation Center at Oregon State University for its hospitality during the completion of this work. We also thank Professor Walter Loveland for providing us with computer facilities. Part of the numerical calculations were performed using the computer facilities of Shiraz University, College of Sciences. One of the authors (A.N.B) thanks the support of Shiraz University during his sabbatical leave at OSU.

[1] A.A. Katsanos, R.W. Shaw, Jr., and R. Vandenbosch, Phys. Rev. C **1**, 594 (1970).
[2] H. Vonach and M. Hille, Nucl. Phys. **A127**, 268 (1969).
[3] S.M. Grimes, Phys. Rev. C **42**, 2744 (1990).
[4] H.A. Bethe, Phys. Rev. **50**, 332 (1937); Rev. Mod. Phys. **9**, 69 (1937).
[5] T. Von Egidy, A.N. Behkami, and H.H. Schmidt, Nucl. Phys. **A454**, 109 (1986).
[6] T. Von Egidy, H.H. Schmidt, and A.N. Behkami, Nucl. Phys. **A481**, 189 (1988).
[7] S. Shlomo and J.B. Natowitz, Phys. Lett. B **252**, 187 (1990).
[8] I.N. De, S. Shlomo, and S.K. Samaddar, Phys. Rev. C **57**, 1398 (1998).
[9] B.K. Agrawal and A. Ansari, Phys. Lett. B **339**, 7 (1994).
[10] S. Shlomo, Nucl. Phys. **A539**, 17 (1992).
[11] S. Shlomo, V.M. Kolomietz, and H. Dejbakhsh, Phys. Rev. C **55**, 1972 (1997).
[12] G.H. Lang, C.W. Johnson, S.E. Koonin, and W.E. Ormand, Phys. Rev. C **48**, 1518 (1993), and references therein.
[13] S.E. Koonin, D.J. Dean, and K. Langanke, Phys. Rep. **278**, 1 (1997).
[14] G. Puddu, P.F. Bortignon, and R.A. Broglia, Phys. Rev. C **42**, R1830 (1990).
[15] A.N. Behkami and Z. Kargar, J. Nucl. Part. Phys. **18**, 1123 (1992).
[16] J.R. Huizenga, A.N. Behkami, J.S. Sventek, and R.W. Atcher, Nucl. Phys. **A223**, 577 (1974).
[17] S. Shlomo and J.B. Natowitz, Phys. Rev. C **44**, 2878 (1991).
[18] S.G. Nilsson *et al.*, Nucl. Phys. **A131**, 1 (1969).

[19] P.A. Seeger and W.M. Howard, Nucl. Phys. **A238**, 491 (1975).
[20] J.R. Nix *et al.*, Nucl. Phys. **A476**, 1 (1988).
[21] P. Moller and J.R. Nix, Nucl. Phys. **A536**, 20 (1992).
[22] A.V. Ignatyuk, G.N. Smirenkin, and A.S. Tishin, Yad. Fiz. **21**, 485 (1975) [Sov. J. Nucl. Phys. **21**, 255 (1975)].
[23] Po-lin Huang, S.M. Grimes, and T.N. Massey, Phys. Rev. C **62**, 024002 (2000).
[24] J.P. Lestone, Phys. Rev. C **52**, 1118 (1995).
[25] Bency John, R.K. Choudhury, B.K. Nayak, A. Saxena, and D.C. Biswas, Phys. Rev. C **63**, 054301 (2001).
[26] M. Guttormsen, M. Hjorth-Jensen, E. Melby, J. Rekstad, A. Schiller, and S. Siem, Phys. Rev. C **64**, 034319 (2001).